

On the Importance of Well-Defined Thermal Correlation Functions in Simulating Vibronic Spectra

Rami Gherib,^{*} Scott N. Genin, and Ilya G. Ryabinkin^{*}

OTI Lumionics Inc., 3415 American Drive Unit 1, Mississauga, Ontario L4V 1T4, Canada

E-mail: rami.gherib@otilumionics.com; ilya.ryabinkin@otilumionics.com

Abstract

Two difficulties associated with the computations of thermal vibrational correlation functions are discussed. The first one is the lack of a well-behaved expression that is valid at both high-temperature and $T \rightarrow 0$ K limits. Specifically, if the partition function and the propagator are considered separately, then thermal vibrational correlation functions may have an indeterminate form $0/0$ in the limit $T \rightarrow 0$ K. This difficulty is resolved when the partition function and the propagator are jointly considered in the harmonic approximation, which allows a problematic term that emanates from the zero-point energy to be cancelled out thereby producing a thermal correlation function with a determinate form in $T \rightarrow 0$ K limit. The second difficulty is related to the multivaluedness of the vibrational correlation function. We show numerically that an improper selection of branch leads to discontinuities in the computed correlation function and an incorrect vibronic spectra. We propose a phase tracking procedure that ensures continuity of both real and imaginary parts of the correlation function to recover the correct spectra. We support our findings by simulating the UV-vis absorption spectra of pentacene at 4 K and benzene at 298 K. Both are found to be in good agreement with their experimental counterparts.

1 Introduction

In silico design of light emitting materials is one of the major applications of computational spectroscopy. Reliable predictions of line positions and shapes in fluorescence and phosphorescence spectra are in demand for identifying promising molecules among thousands and sometimes tens of thousands candidates.

Simulations of vibrationally resolved electronic spectra can be broadly classified as time-independent (TI)¹⁻⁴ or time-dependent (TD).⁵⁻¹⁰ In TI approaches, spectra are simulated as superposition of individual vibronic transitions, often broadened phenomenologically to match experiments. TI methods become impractical for large molecules due to the pro-

hibitively large number of contributing vibronic transitions.¹¹ The extensive computational costs have even prompted some researchers to tackle the problem via quantum computing, particularly via boson sampling and to rethink the computational hardware that ought to be used for such problems.¹² In TD approaches, vibronic spectra are computed by the Fourier transform of the transition dipole correlation function.

When vibronic transitions are considered, TI and TD formalisms require at least two potential energy surfaces (PESs) — one for the initial and another for the final electronic state. Because the construction of fully anharmonic multidimensional PESs is challenging for all but the smallest molecules,¹³ numerous TI and TD approaches rely on the harmonic approximation (HA) in which the true PESs are approximated by multidimensional paraboloids that are constructed from truncated Taylor expansions at relevant nuclear configurations. The relative position and orientation of two paraboloids can be defined through the first-order Duschinsky transformation.¹⁴ Under the umbrella of the HA, additional approximations can be made depending on the choice of reference nuclear geometries where Taylor expansion is made. For example, an adiabatic Hessian model evaluates the final electronic state Hessian at a minimum of the final electronic state, whereas in a vertical Hessian model, the minimum of the initial electronic state is used.^{15–18} Further approximations, such as the independent mode displaced harmonic approximation,¹⁹ neglect Duschinsky rotation and/or assume that the initial and final states have identical harmonic frequencies.

Numerous studies^{6–9,18,20–22} have applied the TD formalism in conjunction with the HA. For rigid molecules, this is a viable alternative to methods that perform on-the-fly dynamical propagations, as they often require expensive electronic structure calculations to be done at every time step and Hessians to be re-evaluated multiple times.^{10,23} A popular and quite successful approach is to use the propagator of a quantum harmonic oscillator in the coordinate basis, the so-called Mehler kernel, to evaluate the transition dipole correlation function analytically. Though some studies^{6,8,18} have derived an expression that incorporates thermal effects (herein referred to as μ_T), others^{22,24} have neglected temperature dependence

and derived it exclusively at 0 K (μ_0). Though one might reasonably expect μ_T to converge smoothly to μ_0 when $T \rightarrow 0$ K, this is not the case since μ_T becomes ill-defined in this limit. μ_T is commonly expressed as a fraction where the Mehler kernel is in the numerator and the partition function is in the denominator and both approach 0 as $T \rightarrow 0$ K, leading to an indeterminate form 0/0 and causes numerical instabilities at extremely low temperatures. To circumvent the issue, de Souza et al.⁹ suggested to redefine certain terms in μ_T at temperatures lower than 10 K such that it would coincide with μ_0 . Doing so, one effectively gets two separate expressions: one used at very low temperatures (less than 10 K) and another used everywhere else. Although this solution is acceptable, because one does not expect to see noticeable differences in spectra taken in the 0 K to 10 K interval, a deeper understanding of the cause of the issue as well as potential consequences are highly desired.

Quantum dynamics of one-dimensional harmonic oscillators that uses the Mehler kernel exhibits occasional time-discontinuities and sudden phase jumps.^{25–27} This feature is well documented and explained in many textbooks that introduce the path-integral formalism.^{28–30} Given that $\mu_T(t)$ corresponding to two multidimensional harmonic oscillators is built from several single-mode propagators, one expects these discontinuities to impact vibronic spectra simulations. Thus, it seems natural to assess such impact and develop a method that delivers continuous $\mu_T(t)$. While one may argue that because such discontinuities do not arise in quantum dynamics obtained by solving the time-dependent Schrödinger equation, that the use of the Mehler kernel ought to be discarded; the propagator approach should be preserved as it allows for easy consideration of thermal effects.

This paper is organized as follows. We begin by introducing key equations used to simulate vibronic spectra within the time-dependent approach. Next, we show how terms inside $\mu_T(t)$ can be factored and canceled out under the HA to yield a well-behaved expression at $T \rightarrow 0$ K. For the sake of simplicity, we analyze the one-dimensional model first before deriving an expression for the thermal vibrational correlation function of a multidimensional harmonic oscillator. After that, we look into the time-discontinuity of $\mu_T(t)$ and propose a

phase tracking scheme that effectively amounts to the inclusion of a *Maslov correction*²⁵ for all individual normal modes. The result is a formula for thermal transition dipole correlation function that is well-defined across all temperatures, time-continuous, and numerically stable. It can be computed for relatively large molecules while fully accounting for Duschinsky rotations and displacements within the adiabatic Hessian model. We illustrate our developments by simulating absorption spectra of pentacene at 4 K in the Franck–Condon approximation and benzene at 298 K in the Herzberg–Teller approximation and compare them with their experimental counterparts. Atomic units are used throughout the paper.

2 Theory

2.1 Vibronic spectra in the time-domain

For the processes that are of interest herein, we apply the semiclassical approach wherein light is described classically and molecules quantum mechanically. The rates of transitions between discrete states can be approximated from perturbation theory by using the state-to-state form of Fermi’s golden rule³¹ and invoking the dipole approximation. The resulting absorption cross section $\sigma_T(\omega)$ for transitions from a set of initially occupied molecular states $\{|\varphi_i\rangle\}$ at thermal equilibrium to a set of states $\{|\varphi_f\rangle\}$ can be given by the following formula^{18,21,28,32}

$$\sigma_T(\omega) = \frac{4\pi^2\omega}{3c} \sum_{i,f} P_i |\langle \varphi_i | \hat{\mu}_M | \varphi_f \rangle|^2 \delta(\omega - \omega_{fi}), \quad (1)$$

where c is the speed of light, $P_i(T) = e^{-\frac{E_i}{k_\beta T}}/Z(T)$ is the Boltzmann population of the initial state at temperature T , k_β is the Boltzmann constant, $Z(T)$ is the system’s partition function, $\hat{\mu}_M$ is the molecular dipole operator and $\delta(\omega - \omega_{fi})$ is a Dirac delta function where $\omega_{fi} = (E_f - E_i)$ is the excitation energy.

In the Born-Oppenheimer approximation, the molecular initial and final quantum states are factorized as $\phi_I(\mathbf{r}|\mathbf{R})\chi_i(\mathbf{R})$ and $\phi_F(\mathbf{r}|\mathbf{R})\chi_f(\mathbf{R})$, respectively. Here, \mathbf{r} are the electronic

and \mathbf{R} are the nuclear coordinates; capitalized subscripts denote electronic, while the lowercase subscripts denote nuclear states. Because we are only interested in the vibrational states, from hereon $\chi_f(\mathbf{R})$ corresponds with the vibrational part of the nuclear state and \mathbf{R} are nuclear internal degrees of freedom.

The quantum transitions amplitudes $\langle \varphi_i | \hat{\mu}_M | \varphi_f \rangle$ are the matrix elements of the molecular dipole operator

$$\hat{\mu}_M(\mathbf{r}, \mathbf{R}) = \hat{\mu}_e(\mathbf{r}) + \hat{\mu}_N(\mathbf{R}), \quad (2)$$

where $\hat{\mu}_e(\mathbf{r})$ and $\hat{\mu}_N(\mathbf{R})$ are the electronic and nuclear dipole moment operators, respectively.

Assuming the Born-Oppenheimer factorization, the electronic degrees of freedom can be integrated out to leave

$$\left| \langle \phi_I \chi_i | \hat{\mu}_M | \phi_F \chi_f \rangle_{\mathbf{r}\mathbf{R}} \right|^2 = \left| \langle \chi_i | \vec{\gamma}_{IF} | \chi_f \rangle_{\mathbf{R}} \right|^2, \quad (3)$$

where

$$\vec{\gamma}_{IF}(\mathbf{R}) = \langle \phi_I | \hat{\mu}_e | \phi_F \rangle_{\mathbf{r}} \quad (4)$$

is the electronic transition dipole moment function and $\langle \cdots \rangle_{\mathbf{R}}$ and $\langle \cdots \rangle_{\mathbf{r}}$ denotes integration over \mathbf{R} and \mathbf{r} , respectively. Note that $\hat{\mu}_N$ does not contribute due the orthogonality of electronic state within the Born-Oppenheimer approximation. In what follows, we suppress the subscripts in $\vec{\gamma}_{IF}$ assuming the initial and final electronic state remain fixed.

The transition dipole moment function is a three dimensional vector whose components are functions of nuclear geometry, $\vec{\gamma}^T(\mathbf{R}) = [\gamma_x(\mathbf{R}), \gamma_y(\mathbf{R}), \gamma_z(\mathbf{R})]$. Its evaluation is simplified through the Condon approximation, where we expand each component of $\vec{\gamma}(\mathbf{R})$ around a potential energy minimum \mathbf{R}_0 in Taylor series and truncate to first order,

$$\vec{\gamma}(\mathbf{R}) \approx \vec{\gamma}(\mathbf{R}_0) + \nabla^T \vec{\gamma}(\mathbf{R}_0)(\mathbf{R} - \mathbf{R}_0), \quad (5)$$

where

$$\nabla^T \vec{\gamma}(\mathbf{R}_0) = \begin{bmatrix} \frac{\partial \gamma_x(\mathbf{R})}{\partial R_1} & \frac{\partial \gamma_x(\mathbf{R})}{\partial R_2} & \cdots & \frac{\partial \gamma_x(\mathbf{R})}{\partial R_N} \\ \frac{\partial \gamma_y(\mathbf{R})}{\partial R_1} & \frac{\partial \gamma_y(\mathbf{R})}{\partial R_2} & \cdots & \frac{\partial \gamma_y(\mathbf{R})}{\partial R_N} \\ \frac{\partial \gamma_z(\mathbf{R})}{\partial R_1} & \frac{\partial \gamma_z(\mathbf{R})}{\partial R_2} & \cdots & \frac{\partial \gamma_z(\mathbf{R})}{\partial R_N} \end{bmatrix} \quad (6)$$

and N denotes the number of vibrational degrees of freedom.

Plugging this expansion into Eq. (3), one can approximate $|\langle \chi_i | \vec{\gamma} | \chi_f \rangle_{\mathbf{R}}|^2$ as the sums of three contributions

$$|\langle \chi_i | \vec{\gamma} | \chi_f \rangle_{\mathbf{R}}|^2 = \rho_{if}^{\text{FC}} + \rho_{if}^{\text{FCHT}} + \rho_{if}^{\text{HT}}, \quad (7)$$

where

$$\rho_{if}^{\text{FC}} = \vec{\gamma}^T(\mathbf{R}_0) \cdot \vec{\gamma}(\mathbf{R}_0) |\langle \chi_i | \chi_f \rangle_{\mathbf{R}}|^2, \quad (8)$$

$$\rho_{if}^{\text{FCHT}} = 2 \vec{\gamma}^T(\mathbf{R}_0) \nabla^T \vec{\gamma}(\mathbf{R}_0) \langle \chi_i | \chi_f \rangle_{\mathbf{R}} \langle \chi_f | \mathbf{R} - \mathbf{R}_0 | \chi_i \rangle_{\mathbf{R}}, \quad (9)$$

$$\rho_{if}^{\text{HT}} = \langle \chi_f | \mathbf{R} - \mathbf{R}_0 | \chi_i \rangle_{\mathbf{R}}^T \nabla \vec{\gamma}^T(\mathbf{R}_0) \nabla^T \vec{\gamma}(\mathbf{R}_0) \langle \chi_f | \mathbf{R} - \mathbf{R}_0 | \chi_i \rangle_{\mathbf{R}} \quad (10)$$

and the nuclear states $\chi(\mathbf{R})$ are real functions. The superscripts FC, FCHT and HT in the previous equations refer to Franck–Condon, Franck–Condon Herberg–Teller and Herzberg–Teller terms, respectively.

By substituting Eq. (7) and the Dirac delta function as a Fourier transform $\delta(\omega) = \frac{1}{2\pi} \int_{-\infty}^{\infty} e^{i\omega t} dt$ into Eq. (1), the spectra is defined in the time domain^{6–8}

$$\sigma_T(\omega) = \frac{2\pi\omega}{3c} \text{Re} \int_0^{\infty} e^{i\omega t} (\mu_T^{\text{FC}}(t) + \mu_T^{\text{FCHT}}(t) + \mu_T^{\text{HT}}(t)) dt, \quad (11)$$

where

$$\mu_T^{\text{FC}}(t) = \sum_{i,f} \frac{1}{Z_I} \rho_{if}^{\text{FC}} e^{-iE_i\tau} e^{-iE_ft}, \quad (12)$$

$$\mu_T^{\text{FCHT}}(t) = \sum_{i,f} \frac{1}{Z_I} \rho_{if}^{\text{FCHT}} e^{-iE_i\tau} e^{-iE_ft}, \quad (13)$$

$$\mu_T^{\text{HT}}(t) = \sum_{i,f} \frac{1}{Z_I} \rho_{if}^{\text{HT}} e^{-iE_i\tau} e^{-iE_ft} \quad (14)$$

are hereon referred to as FC, FCHT and HT correlation functions, respectively and $\tau = \frac{-i}{k_\beta T} - t$.

2.2 $\mu_T^{\text{FC}}(t)$ at low temperature

The analytical expression for $\mu_T^{\text{FC}}(t)$ can be represented in the continuous basis (see details in Appendix A) as

$$\mu_T^{\text{FC}}(t) = \vec{\gamma}^\top(\mathbf{R}_0) \cdot \vec{\gamma}(\mathbf{R}_0) \tilde{\mu}_T^{\text{FC}}(t), \quad (15)$$

where

$$\tilde{\mu}_T^{\text{FC}}(t) = \int \frac{1}{Z_I} \langle \mathbf{R}' | e^{-i\hat{H}_I\tau} | \mathbf{R} \rangle \langle \mathbf{R} | e^{-i\hat{H}_F t} | \mathbf{R}' \rangle d\mathbf{R} d\mathbf{R}'. \quad (16)$$

Before continuing with multidimensional cases, we turn our attention to the generic one-dimensional harmonic oscillator. We denote the spatial variable of the one-dimensional harmonic oscillator as q , its frequency as w , its mass as m , and we can evaluate its $\tilde{\mu}_T^{\text{FC}}(t)$ as per Eq. (16) using the partition function

$$Z_I(T) = \frac{e^{-\frac{w}{2k_\beta T}}}{1 - e^{-\frac{w}{k_\beta T}}} = \frac{1}{2 \sinh\left(\frac{w}{2k_\beta T}\right)}, \quad (17)$$

and the propagator in the position basis $\langle q | e^{-i\hat{H}t} | q' \rangle$ also known as the ‘‘Mehler kernel,’’

which has the well-known form³⁰

$$\langle q|e^{-i\hat{H}t}|q'\rangle = \sqrt{\frac{m}{2\pi i}} \sqrt{\frac{w}{\sin(wt)}} e^{\left(imw \left(\frac{(q^2+q'^2)\cot(wt)}{2} - \frac{qq'}{\sin(wt)} \right) \right)}. \quad (18)$$

In the limit $T \rightarrow 0$ K, both $Z_I(T)$ and $\langle q|e^{-i\hat{H}\tau}|q'\rangle$ converge to 0. In the Mehler kernel, this behavior is due to its pre-exponential factor

$$\sqrt{\frac{1}{2i \sin(w\tau)}} = \frac{e^{\frac{iwt}{2}} e^{-\frac{w}{2k\beta T}}}{\sqrt{1 - e^{-2iw\tau}}}. \quad (19)$$

As written, $\lim_{T \rightarrow 0} \frac{\langle q|e^{-i\hat{H}t}|q'\rangle}{Z(T)}$ has an indeterminate form 0/0. This is not only a conceptual problem, but it also makes computations susceptible to numerical instabilities at extremely low temperatures.

To circumvent this issue, some studies (e.g. Ref. 9) have employed two different expressions for $\mu_T^{\text{FC}}(t)$. One is intended for high temperatures where one does not encounter the aforementioned numerical issues and coincides with the derivations presented so far. Another is meant for temperatures near 0 K and is derived from Eq. (1) but with the sum extending only through the vibrational states of the final electronic state, which effectively assumes that the initial state is entirely populated by the ground vibrational state.

We propose a well-defined expression for $\mu_T^{\text{FC}}(t)$, namely by evaluating the determinate form of the quotient $\tilde{K}_I(q, q', \tau)$,

$$\tilde{K}_I(q, q', \tau) = \frac{\langle q|e^{-i\hat{H}_I\tau}|q'\rangle}{Z_I} \quad (20)$$

$$= \sqrt{\frac{w_I}{\pi}} \frac{\left(1 - e^{-\frac{w_I}{k\beta T}}\right) e^{\frac{iw_I\tau}{2}}}{\sqrt{1 - e^{-2iw_I\tau}}} e^{\left(iw_I \left(\frac{(q^2+q'^2)\cot(w_I\tau)}{2} - \frac{qq'}{\sin(w_I\tau)} \right) \right)} \quad (21)$$

in which the term $e^{-\frac{w}{2k\beta T}}$ is canceled out in both $Z_I(T)$ and $\langle q|e^{-i\hat{H}\tau}|q'\rangle$. Substituting Eq. (21) into Eq. (16) yields an expression of the FC correlation function that is well-defined

at low-temperatures

$$\bar{\mu}_T^{\text{FC}}(t) = \vec{\gamma}^\top(q_0) \cdot \vec{\gamma}(q_0) \int \tilde{K}_I(q', q, \tau) \langle q | e^{-i\hat{H}_F t} | q' \rangle dq dq'. \quad (22)$$

It is worth noting that one can also *partially* derive Eq. (21) by neglecting or removing the zero-point energy in the Mehler kernel and in $Z_I(T)$. We can do so by multiplying both expressions by $e^{iE_0^{\text{HO}}t}$ where E_0^{HO} is the zero-point energy of the harmonic oscillator,

$$K_{\text{noZPE}}(q, q', t) = e^{iE_0^{\text{HO}}t} \langle q | e^{-i\hat{H}t} | q' \rangle \quad (23)$$

$$= \sqrt{\frac{mw}{\pi}} \frac{1}{\sqrt{1 - e^{-2iwt}}} e^{(imw(\frac{\cot(wt)}{2}(q^2 + q'^2) - \frac{1}{\sin(wt)}qq')),} \quad (24)$$

$$Z_{\text{noZPE}}(T) = e^{\frac{E_0^{\text{HO}}}{k_\beta T}} Z(T) \quad (25)$$

$$= \frac{1}{1 - e^{-\frac{w}{k_\beta T}}}, \quad (26)$$

so that

$$\tilde{K}(q, q', \tau) = e^{iE_0 t} \frac{K_{\text{noZPE}}(q, q', \tau)}{Z_{\text{noZPE}}(T)}, \quad (27)$$

thereby making the quotient of K_{noZPE} and Z_{noZPE} differs from \tilde{K} by a global phase. This phase does not alter the spectral line shape, it merely shifts it horizontally by E_0^{HO} along the energy axis.

The issue of the indeterminate form of $\lim_{T \rightarrow 0} \frac{\langle q | e^{-i\hat{H}\tau} | q' \rangle}{Z(T)}$ is general as it is not limited to the harmonic oscillator model and arises in all bounded systems. The generic forms of $\langle q | e^{-i\hat{H}t} | q' \rangle$ and $Z(T)$ for any bounded system can be expressed in the eigenbasis $\{\phi_n(q)\}$ and energy spectrum $\{E_n\}$ of the Hamiltonian

$$\langle q | e^{-i\hat{H}\tau} | q' \rangle = e^{-\frac{E_0}{k_\beta T}} e^{-iE_0 t} \sum_n e^{i\Delta E_n \tau} \phi_n^*(q) \phi_n(q'), \quad (28)$$

$$Z(T) = e^{-\frac{E_0}{k_\beta T}} \sum_n e^{-\frac{\Delta E_n}{k_\beta T}}, \quad (29)$$

where E_0 is the system's zero point energy, ΔE_n is the energy difference between E_n and E_0 and $\lim_{T \rightarrow 0} e^{-\frac{E_0}{k\beta T}} \rightarrow 0$. As a result, Eq. (23), Eq. (25) and Eq. (27) are general equations in the sense that they are valid to all bounded systems — one only needs to replace E_0^{HO} with E_0 . These equations used in conjunction with Eq. (22) can effectively yield Franck-Condon correlation functions with a determinate forms. Moreover, it is evident that when partition functions and propagators are obtained approximately, that the cancellation in Eq. (27) only works if both entail the exact same zero-point energy.

2.3 $\tilde{\mu}_T^{\text{FC}}(t)$ in the multidimensional case

Eq. (18), may be re-expressed more succinctly in mass-weighted coordinates as

$$K(q, q', t) = \sqrt{\frac{a}{2\pi i}} e^{\left(\frac{i}{2} \begin{bmatrix} q & q' \end{bmatrix} \begin{bmatrix} b & -a \\ -a & b \end{bmatrix} \begin{bmatrix} q \\ q' \end{bmatrix} \right)} \quad (30)$$

where $a = \frac{w}{\sin(wt)}$ and $b = \frac{w}{\tan(wt)}$. In the case of a N -dimensional harmonic oscillator, if one works in the basis of normal modes \mathbf{Q} , the Hamiltonian can be expressed as the sum of N one-dimensional Hamiltonians. The corresponding N -dimensional propagator is thus the product of one-dimensional ones,

$$\begin{aligned} K(\mathbf{Q}, \mathbf{Q}', t) &= \prod_{n=1}^N K_n(q_n, q'_n, t) \\ &= \sqrt{\frac{\det(\mathbf{A})}{(2\pi i)^N}} e^{\left(\frac{i}{2} \begin{bmatrix} \mathbf{Q} & \mathbf{Q}' \end{bmatrix} \begin{bmatrix} \mathbf{B} & -\mathbf{A} \\ -\mathbf{A} & \mathbf{B} \end{bmatrix} \begin{bmatrix} \mathbf{Q} \\ \mathbf{Q}' \end{bmatrix} \right)} \end{aligned} \quad (31)$$

where \mathbf{A} and \mathbf{B} are diagonal matrices with elements $A_n = \frac{w_n}{\sin(w_n t)}$ and $B_n = \frac{w_n}{\tan(w_n t)}$, respectively. In the case of $\tilde{K}(\mathbf{Q}, \mathbf{Q}', \tau)$, one obtains a similar expression but with a different

pre-exponential factor,

$$\tilde{K}(\mathbf{Q}, \mathbf{Q}', t) = \det(\mathbf{\Omega}) e^{\left(\frac{i}{2} \begin{bmatrix} \mathbf{Q} & \mathbf{Q}' \end{bmatrix} \begin{bmatrix} \mathbf{B} & -\mathbf{A} \\ -\mathbf{A} & \mathbf{B} \end{bmatrix} \begin{bmatrix} \mathbf{Q} \\ \mathbf{Q}' \end{bmatrix} \right)} \quad (32)$$

where $\mathbf{\Omega}$ is a diagonal matrix with elements $\Omega_n = \sqrt{\frac{w_n}{\pi}} \frac{(1 - e^{-w_n \beta}) e^{\frac{i w_n t}{2}}}{\sqrt{1 - e^{2 i w_n t} e^{-2 w_n \beta}}}$.

For molecules under the HA, nuclear degrees of freedom are often represented in the basis of normal modes. Those coincide with the eigenvectors of mass-weighted Hessians of either initial or final electronic states, which are denoted by $\mathbf{\Lambda}_I$ and $\mathbf{\Lambda}_F$, respectively. Given an initial nuclear configuration expressed in the basis of normal modes of the final electronic state \mathbf{Q}_F , a change in basis to the normal modes of the initial electronic state \mathbf{Q}_I can be done via the Duschinsky transformation

$$\mathbf{Q}_I = \mathbf{J}_{IF} \mathbf{Q}_F + \mathbf{K} \quad (33)$$

where $\mathbf{J}_{IF} = \mathbf{\Lambda}_I^\top \mathbf{\Lambda}_F$ and $\mathbf{K} = \mathbf{\Lambda}_I^\top \mathbf{L}_F$ with \mathbf{L}_F being the nuclear displacement of the final state PES minimum expressed in mass-weighted Cartesian coordinates.

Ultimately, by solving the integral resulting from the insertion of Eq. (31) and Eq. (32) into multidimensional analogue of Eq. (22) and the change of variables as per Eq. (33), we get

$$\bar{\mu}_T^{\text{FC}}(t) = \det(\mathbf{\Omega}_I) \sqrt{\frac{(-2\pi i)^N \det(\mathbf{A}_F)}{\det(\mathbf{D})}} e^{i \left(-\frac{\mathbf{E}^\top \mathbf{D}^{-1} \mathbf{E}}{2} + F \right)} \quad (34)$$

where

$$\begin{aligned} \mathbf{D} &= \begin{bmatrix} \mathbf{B}_F + \mathbf{J}_{IF}^\top \mathbf{B}_I \mathbf{J}_{IF} & -(\mathbf{A}_F + \mathbf{J}_{IF}^\top \mathbf{A}_I \mathbf{J}_{IF}) \\ -(\mathbf{A}_F + \mathbf{J}_{IF}^\top \mathbf{A}_I \mathbf{J}_{IF}) & \mathbf{B}_F + \mathbf{J}_{IF}^\top \mathbf{B}_I \mathbf{J}_{IF} \end{bmatrix}, \\ \mathbf{E}^\top &= \begin{bmatrix} \mathbf{K}^\top (\mathbf{B}_I - \mathbf{A}_I) \mathbf{J}_{IF} & \mathbf{K}'^\top (\mathbf{B}_I - \mathbf{A}_I) \mathbf{J}_{IF} \end{bmatrix}, \\ F &= \mathbf{K}'^\top (\mathbf{B}_I - \mathbf{A}_I) \mathbf{K} \end{aligned} \quad (35)$$

For large molecules, the determinants in Eq. (34) may acquire large magnitudes and their

computations may result in overflow errors. Thus, to compute $\mu_T^{\text{FC}}(t)$ of large molecules, it is necessary to reexpress the pre-exponential factor in a more tractable form. Looking at Eq. (34), one may be tempted to compute $\det(\mathbf{\Omega}_I^2 \mathbf{A}_F \mathbf{D}^{-1})$ and expect a numerical outcome whose magnitude is close to 1, given that the matrix elements of $\mathbf{\Omega}_I^2 \mathbf{A}_F$ are of approximately the same order of magnitude as those of \mathbf{D} . However, this cannot be done because \mathbf{D} is a $2N \times 2N$ matrix and $\mathbf{\Omega}_I$ and \mathbf{A}_F are $N \times N$ matrices.

To proceed forward approximately along this path, we need to define an $N \times N$ matrix whose determinant equals that of \mathbf{D} . Such matrix is $\tilde{\mathbf{D}} = \mathbf{D}_{11} (\mathbf{D}_{11} - \mathbf{D}_{12} \mathbf{D}_{11}^{-1} \mathbf{D}_{12})$, which is constructed from the submatrices of \mathbf{D} where $\mathbf{D}_{11} = (\mathbf{B}_F + \mathbf{J}_{IF}^\top \mathbf{B}_I \mathbf{J}_{IF})$, $\mathbf{D}_{12} = -(\mathbf{A}_F + \mathbf{J}_{IF}^\top \mathbf{A}_I \mathbf{J}_{IF})$ and satisfies $\det(\mathbf{D}) = \det(\tilde{\mathbf{D}})$ and $(\det(\mathbf{D}))^{-1} = \det(\tilde{\mathbf{D}}^{-1})$.^{9,33} Furthermore, to ensure that the use of $\sqrt{\det(\mathbf{\Omega}_I^2)}$ gives the same result as that of $\det\{\mathbf{\Omega}_I\}$, we introduce η that equals either +1 or -1 such that $\det(\mathbf{\Omega}_I) = \eta \sqrt{\det(\mathbf{\Omega}_I^2)}$. The substitution of these terms inside Eq. (34) yields

$$\bar{\mu}_T^{\text{FC}}(t) = \eta(-2\pi i)^{\frac{N}{2}} \sqrt{\det(\mathbf{\Omega}_I^2 \mathbf{A}_F \tilde{\mathbf{D}}^{-1})} e^{i\left(-\frac{\mathbf{E}^\top \mathbf{D}^{-1} \mathbf{E}}{2} + F\right)}, \quad (36)$$

which is a numerically more stable than Eq. (34).

2.4 Time-discontinuity in $\tilde{\mu}_T^{\text{FC}}(t)$

A direct numerical implementation of Eq. (36) yields a discontinuous $\bar{\mu}_T^{\text{FC}}(t)$ and an erroneous vibronic spectrum. The source of the time-discontinuity is the pre-exponential factor. The term under the square root is a complex-valued function of time, $|S(t)|e^{i\theta(t)}$ and has two square roots: $\sqrt{|S(t)|}e^{i\frac{\theta(t)}{2}}$ and $\sqrt{|S(t)|}e^{i(\frac{\theta(t)}{2}+\pi)}$. When a square root is computed, most numerical libraries output the principal value, which is usually the root with the positive real component. Such choice is not always valid.

Fundamentally, the discontinuity arises because the expression used for the one-dimensional harmonic oscillator propagator, Eq. (18), can be discontinuous in time; it is multiplied by

$\frac{1}{\sqrt{-1}} = e^{-i\pi/2}$ after half-period increments.²⁶ In the path integral (PI) formalism, these extra phase jumps stem from the contributions of variations surrounding classical trajectories; see Appendix D for the detailed explanation.

To correct for the discontinuity in the one-dimensional harmonic oscillator propagator, it is common to employ the *Maslov phase correction*.²⁵ This correction consists in adopting the following expression for the Mehler kernel instead of Eq. (18):

$$\langle q|e^{-i\hat{H}t}|q'\rangle = \sqrt{\frac{m}{2\pi i}} \sqrt{\frac{w}{|\sin(wt)|}} e^{\left(imw\left(\frac{(q^2+q'^2)}{2}\cot(wt) - \frac{qq'}{|\sin(wt)|}\right)\right)} e^{\frac{-i\nu\pi}{2}}, \quad (37)$$

where ν is called the *Morse index* and it is the number of elapsed half-periods in the time span $[0, t]$.^{28–30} In deriving $\mu_T^{\text{FC}}(t)$ of a multidimensional harmonic oscillator, one could have begun with Eq. (37) rather than Eq. (18). This would have produced an expression analogous to Eq. (36) that would have included $e^{\frac{-i\nu\pi}{2}}$ terms for every initial and final electronic state normal modes. Such an approach would have had the advantage of preventing the time-discontinuity issue. The disadvantage, however, is that one would have had to keep track of all Morse indexes and evolve them over the course of the dynamics, thereby making the entire procedure cumbersome and error prone. Instead, we propose an alternative approach of tracking the *total* phase. We multiply the right-hand side of Eq. (36) with a real phase factor $\theta(t)$. This phase factor will equal either 1 or -1 , depending on which value minimizes the difference between $\mu_T^{\text{FC}}(t)$ values at consecutive time steps. This effectively allows one to select the appropriate branch of $z^{\frac{1}{2}}$ and to ensure the continuity of real and imaginary parts of $\mu_T^{\text{FC}}(t)$, which, as we will show in Sec. 3.2, is paramount to vibronic spectra simulations. The inclusion of the phase factor yields a final expression for the FC correlation function

$$\tilde{\mu}_T^{\text{FC}}(t) = \theta\eta(-2\pi i)^{\frac{N}{2}} \sqrt{\det\left(\Omega_I^2 \mathbf{A}_F \tilde{\mathbf{D}}^{-1}\right)} e^{\left(i\left(-\frac{\mathbf{E}^T \mathbf{D}^{-1} \mathbf{E}}{2} + F\right)\right)}, \quad (38)$$

which is applicable for any temperature $T \geq 0$ K, is continuous in time, and is stable numerically for large molecules with many vibrational degrees of freedom. The phase tracking

procedure removes the need to compute the Morse indexes of all normal modes at all time steps. However, assessing the continuity between $\mu_T^{\text{FC}}(t)$ values of adjacent time steps requires that dynamical simulations be performed with sufficiently small time steps.

In the case where several normal modes have the same frequencies, degenerate Hessian eigenvectors are arbitrarily defined. This arbitrariness can find itself in the Duschinsky matrix \mathbf{J}_{IF} of Eq. (33), and in $\tilde{\mu}_T^{\text{FC}}(t)$ of Eq. (38). The degeneracies could cause $\tilde{\mu}_T^{\text{FC}}(t)$ to have an arbitrary phase, which would be unresolved by the phase-tracking procedure herein. In our implementation, we avoid this issue altogether by computing the normal modes once at the start of the dynamics. The Duschinsky matrix is computed once, and it is stored in memory and reused in subsequent time steps. This effectively amounts to fixing the basis of the degenerate subspace.

3 Results and Discussion

3.1 Computational details

We simulated the absorption spectra of pentacene and benzene. Electronic structure calculations were performed using Firefly³⁴ software package. Ground and excited state Hessians and geometries minima were computed at B3LYP/6-311G(df)³⁵⁻³⁷ level of theory. This level of theory is comparable to ones used in other theoretical simulations of vibronic spectral shapes that report good agreement with their experimental counterparts.^{9,18,38} Additionally, it was demonstrated²² that this level of theory produces spectral line shapes similar to those obtained with the second-order approximate coupled-cluster (CC2) method and hybrid functionals used in conjunction with larger basis sets.¹¹

Hessians were computed by first-order numerical differentiation of gradients and atomic coordinate displacements of 0.01 Å. For each Hessian calculation, a total of 3N+1 gradients were evaluated (N here is the number of atoms in the molecule). Excited state calculations were performed with TDDFT in which the first 10 roots were computed. For each molecule,

the lowest singlet excited state was selected as it corresponded to the state of interest.

The total duration of dynamical simulations were 2000 fs with a time step of 0.005 fs. This time step is chosen for the phase tracking procedure to avoid any discontinuities; it is comparable in magnitude to ones used in previous studies; 0.006 fs in Ref. 8 and 0.015 fs in Ref. 9. To model broadening effects stemming from environmental factors present in experiments, $\mu_T^{\text{FC}}(t)$, $\mu_T^{\text{FCHT}}(t)$ and $\mu_T^{\text{HT}}(t)$ are multiplied with an exponential damping function, $f(t) = e^{-\frac{t}{\kappa}}$, where κ is the relaxation time. For pentacene and benzene respectively, we used $\kappa = 138.2$ fs and $\kappa = 40.3$ fs. The discrete Fourier transform was performed using the NumPy suite of numerical libraries.³⁹

3.2 Absorption spectra of pentacene in the Franck–Condon approximation

The vibronic spectra of pentacene has been the subject of numerous studies^{6,22,40,41} and to demonstrate the applicability of Eq. (38) in low temperatures, we compare in Fig. 1 the theoretical spectra of pentacene at 4 K obtained with and without phase correction to its experimental counterpart.⁴¹ Pentacene belongs to the D_{2h} symmetry group and the featured spectra correspond to a $A_g \rightarrow B_{2u}$ transition that is Franck–Condon allowed. The experimental spectrum has been obtained using the matrix-isolation technique where pentacene monomers were trapped in a neon matrix. At low concentrations, this methodology approximates light absorption and emission in the absence of solvation and environmental effects. Thus, DFT and TDDFT calculations were done in vacuum. The phase-corrected theoretical spectrum was shifted by 0.56 eV as to improve correspondence with experiment. The need to shift theoretical spectra stems from the general tendency of B3LYP to overestimating singlet vertical excitations of benzene and acenes by approximately 0.5 eV.^{22,42}

As clearly visible in Fig. 1, absence of phase correction results in a nonsensical spectrum (the red dotted curve). The solid blue line however includes the phase correction for which the branch has been appropriately chosen to render the correlation function continuous in time.

These results indicate that the continuity of real and imaginary components of the simulated correlation function has a dramatic impact on vibronic spectra and that the methodology based on Eq. (38) is in agreement with experiments.

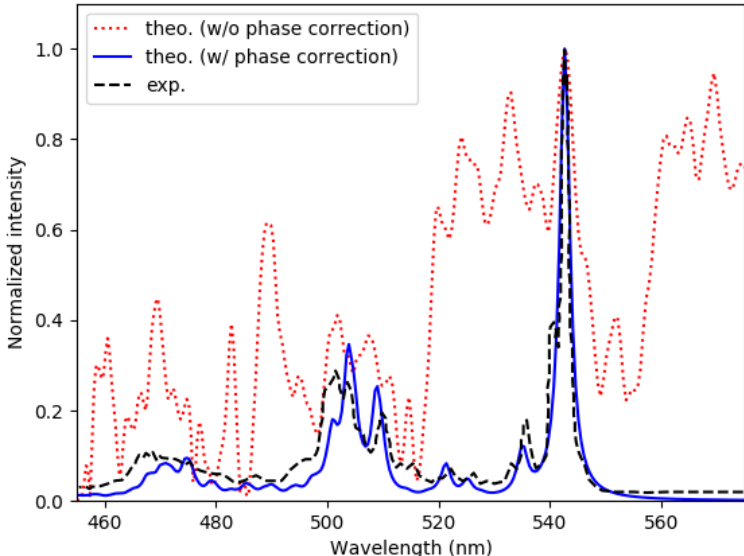


Figure 1: Absorption spectra for pentacene at 4 K. The red dotted line corresponds to a theoretical simulation that does not incorporate phase correction and the solid blue line includes the phase correction. The theoretical spectrum with phase correction was shifted horizontally by 0.56 eV so as to match the experimental spectra.⁴¹

3.3 Absorption spectra of benzene with Herzberg–Teller effects

Benzene and its derivatives are the building blocks of a wide range of organic molecules and have been the subject of numerous investigations.^{9,43–47} Since benzene has D_{6h} symmetry, its lowest energy transition $A_{1g} \rightarrow B_{2u}$ is symmetry-forbidden in the Franck–Condon approximation and the spectra arises solely from the HT correlation function (see Eq. (52) of Appendix C). We present in Fig. 2 the absorption spectra of benzene at 298 K for the purpose of illustrating the application of Eq. (38) (which is necessary to compute $\mu_T^{\text{HT}}(t)$ as shown in Appendix C) at room temperature. In Fig. 2, the theoretical spectrum was shifted by 0.53 eV so as to match the experiment.⁴⁸ Our results seem to be in reasonable agreement

with their experimental counterpart as well as previous theoretical reports.^{9,49}

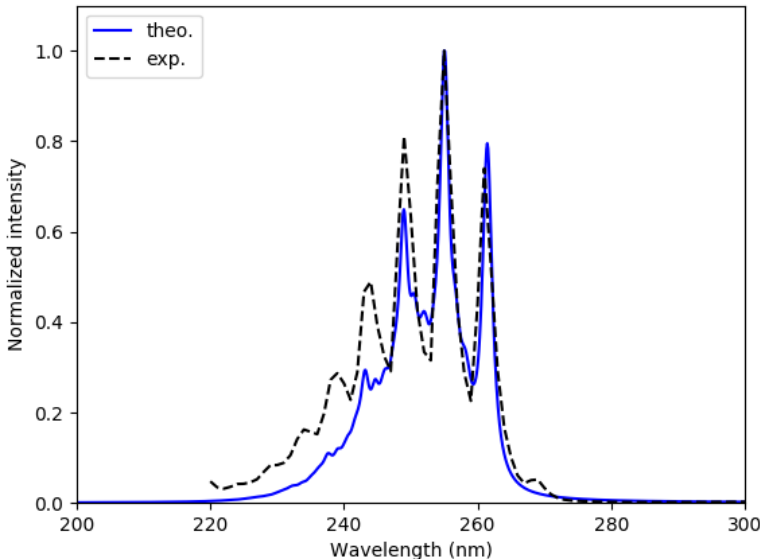


Figure 2: Absorption spectra for benzene in hexane at 298 K. The solid blue line corresponds to a theoretical simulation that includes the phase correction. It was shifted horizontally by 0.53 eV so as to match the experimental spectra.⁴⁸

4 Conclusions

We investigated two complications that may arise while computing thermal vibrational correlation functions in the harmonic approximation. The first complication is that the correlation functions can be ill-defined at extremely low temperatures if the partition function and the Mehler kernel, which are their key components, are considered independently. This is caused by zero-point energy terms present in both the partition function and the propagator. Their removal, either through a cancellation of terms or by neglecting the zero-point energy entirely, yields a thermal correlation function that has a determinate form in the $T \rightarrow 0$ K limit. This provides a means of computing vibronic spectra within the time-dependent formulation that is unified without resorting to consider two disjoint temperature regimes.

The second complication is that thermal vibrational correlation functions in molecular

systems can be discontinuous in time. This occurs because the pre-exponential factor of the Mehler kernel is multivalued. Though one may attempt to construct correlation functions from Maslov-corrected single mode propagators, this would necessitate evolving all underlying Morse indexes during dynamics, which may be cumbersome to implement. Alternatively, as we have shown, the inclusion of a single *global* phase parameter in the final expression of the correlation function suffices to produce a result whose real and imaginary parts are continuous. This phase ultimately selects the appropriate branch of $z^{\frac{1}{2}}$ and minimizes the difference between values of the correlation function of adjacent time steps. While the current work was under review, Begušić et al.²³ published a study that also addressed in part the discontinuity of the correlation function.

By addressing these two complications, we obtained an expression for the thermal dipole autocorrelation function, Eq. (38), that is well-defined and continuous in time. We assessed our findings on two realistic molecular systems, pentacene at 4 K and benzene at 298 K. We found that nonsensical absorption spectra were obtained when phase corrections were omitted (as in the case of pentacene), while with the phase correction our theoretical results matched well with the experimental counterparts.

Although our work focused mostly on harmonic systems, our conclusions are relevant to other models. In any model with positive zero-point energy, one should expect that independent considerations of propagators and partition functions can lead to thermal correlation functions with indeterminate forms in the $T \rightarrow 0$ K limit. In such case, one can resort to the procedure described in Sec. 2.2 to obtain a determinate form. We also expect the time-discontinuity issue to persist in bound anharmonic models whose potential energy surfaces are locally well approximated by quadratic functions and where the underlying dynamics are confined to those regions. This would be the case if the initial and final potential energy surfaces resemble Morse potentials with overlapping minima and large dissociation energies. Furthermore, as it may be difficult to predict analytically the exact instance of the propagator’s sudden phase change in arbitrary potentials, the numerical procedure discussed in

Sec. 2.4 is a general solution for obtaining continuous correlation functions.

A Derivation of the analytical expression of $\mu_T^{\text{FC}}(t)$

By plugging the expression of ρ_{if}^{FC} from Eq. (8) inside that of $\mu_T^{\text{FC}}(t)$ in Eq. (12) we get

$$\mu_T^{\text{FC}}(t) = \vec{\gamma}^\top(\mathbf{R}_0) \cdot \vec{\gamma}(\mathbf{R}_0) \cdot \tilde{\mu}_T^{\text{FC}}(t), \quad (39)$$

where $\tilde{\mu}_T^{\text{FC}}(t)$ is defined as

$$\tilde{\mu}_T^{\text{FC}}(t) = \sum_{i,f} \frac{1}{Z_I} \langle \chi_i | \chi_f \rangle \langle \chi_f | \chi_i \rangle e^{-iE_i\tau} e^{-iE_ft}. \quad (40)$$

By considering that

$$\sum_f e^{-iE_ft} \langle \chi_i | \chi_f \rangle \langle \chi_f | \chi_i \rangle = \langle \chi_i | e^{-i\hat{H}_F t} | \chi_i \rangle, \quad (41)$$

we can rewrite $\tilde{\mu}_T^{\text{FC}}(t)$ as

$$\tilde{\mu}_T^{\text{FC}}(t) = \frac{1}{Z_I} \sum_i e^{-iE_i\tau} \langle \chi_i | e^{-i\hat{H}_F t} | \chi_i \rangle, \quad (42)$$

and through a resolution of the identity $\hat{1} = \int |\mathbf{Q}\rangle \langle \mathbf{Q}| d\mathbf{Q}$ inside the equation above, we get

$$\tilde{\mu}_T^{\text{FC}}(t) = \frac{1}{Z_I} \int \sum_i e^{-iE_i\tau} \langle \chi_i | \mathbf{Q} \rangle \langle \mathbf{Q} | e^{-i\hat{H}_F t} | \mathbf{Q}' \rangle \langle \mathbf{Q}' | \chi_i \rangle d\mathbf{Q} d\mathbf{Q}' \quad (43)$$

whose infinite sum via the spectral representation of $e^{-i\hat{H}_i t} = \sum_i e^{-iE_i t} |\chi_i\rangle \langle \chi_i|$,

$$\tilde{\mu}_T^{\text{FC}}(t) = \frac{1}{Z_I} \int \langle \mathbf{Q}' | e^{-i\hat{H}_I \tau} | \mathbf{Q} \rangle \langle \mathbf{Q} | e^{-i\hat{H}_F t} | \mathbf{Q}' \rangle d\mathbf{Q} d\mathbf{Q}'. \quad (44)$$

B Derivation of the analytical expression of $\mu_T^{\text{FCHT}}(t)$

To derive $\mu_T^{\text{FCHT}}(t)$, we begin by plugging ρ_{if}^{FCHT} from Eq. (8) into $\mu_T^{\text{FCHT}}(t)$ in Eq. (13) such that

$$\mu_T^{\text{FCHT}}(t) = 2\vec{\gamma}^\dagger(\mathbf{R}_0) \cdot \nabla^\dagger \vec{\gamma}(\mathbf{R}_0) \cdot \tilde{\mu}_T^{\text{FCHT}}(t), \quad (45)$$

where

$$\tilde{\mu}_T^{\text{FCHT}}(t) = \sum_{i,f} \frac{1}{Z_I} \langle \chi_i | \chi_f \rangle \langle \chi_f | \hat{\mathbf{R}} - \mathbf{R}_0 | \chi_i \rangle e^{-iE_f t} e^{-iE_i \tau}. \quad (46)$$

We obtain a more compact expression for $\tilde{\mu}_T^{\text{FCHT}}(t)$ by first considering

$$\sum_f \langle \chi_f | \chi_i \rangle \langle \chi_i | (\hat{\mathbf{R}} - \mathbf{R}_0) | \chi_f \rangle e^{-iE_f t} = \langle \chi_i | (\hat{\mathbf{R}} - \mathbf{R}_0) e^{-i\hat{H}_F t} | \chi_i \rangle, \quad (47)$$

such that

$$\begin{aligned} \tilde{\mu}_T^{\text{FCHT}}(t) &= \frac{1}{Z_I} \sum_i e^{-iE_i \tau} \langle \chi_i | (\hat{\mathbf{R}} - \mathbf{R}_0) e^{-i\hat{H}_F t} | \chi_i \rangle \\ &= \int \int \frac{1}{Z_I} \sum_i e^{-iE_i \tau} \langle \chi_i | \mathbf{R} \rangle \langle \mathbf{R} | (\hat{\mathbf{R}} - \mathbf{R}_0) e^{-i\hat{H}_F t} | \mathbf{R}' \rangle \langle \mathbf{R}' | \chi_i \rangle d\mathbf{R} d\mathbf{R}' \\ &= \int \int \frac{1}{Z_I} \left(\int \langle \mathbf{R} | (\hat{\mathbf{R}} - \mathbf{R}_0) | \mathbf{R}'' \rangle \langle \mathbf{R}'' | e^{-i\hat{H}_F t} | \mathbf{R}' \rangle d\mathbf{R}'' \right) \langle \mathbf{R}' | e^{-i\hat{H}_I t} | \mathbf{R} \rangle d\mathbf{R} d\mathbf{R}'. \end{aligned} \quad (48)$$

Given the freedom to Taylor expand $\gamma(\mathbf{R})$ from arbitrary points, one can choose $\mathbf{R}_0 = 0$ and recalling $\langle \mathbf{R} | \hat{\mathbf{R}} | \mathbf{R}'' \rangle = \mathbf{R} \delta(\mathbf{R} - \mathbf{R}'')$ we have

$$\tilde{\mu}_T^{\text{FCHT}}(t) = \int \int \mathbf{R} \langle \mathbf{R} | e^{-i\hat{H}_F t} | \mathbf{R}' \rangle \frac{\langle \mathbf{R}' | e^{-i\hat{H}_I t} | \mathbf{R} \rangle}{Z_I} d\mathbf{R} d\mathbf{R}'. \quad (49)$$

Since \mathbf{R} is an internal nuclear coordinate, it can be replaced in Eq. (49) by the normal modes \mathbf{Q} of relevant PESs computed at their minima. Since the product between the two propagators divided by the partition function was determined in Eq. (34), we can express

Eq. (49) as follows

$$\tilde{\mu}_T^{\text{FCHT}}(t) = \det(\mathbf{\Omega}_I) \sqrt{\frac{\det(\mathbf{A}_F)}{(2\pi i)^N}} \int \int \mathbf{Q}_F e^{\left(\frac{i}{2} \begin{bmatrix} \mathbf{Q}_F & \mathbf{Q}'_F \end{bmatrix} \mathbf{D} \begin{bmatrix} \mathbf{Q}_F \\ \mathbf{Q}'_F \end{bmatrix} + i \mathbf{E}^\top \begin{bmatrix} \mathbf{Q}_F \\ \mathbf{Q}'_F \end{bmatrix} + iF \right)} d\mathbf{Q}_F d\mathbf{Q}'_F. \quad (50)$$

To compute the integral above, we denote $\mathbf{E}^\top = \begin{bmatrix} \mathbf{E}_1^\top & \mathbf{E}_2^\top \end{bmatrix}$ where $\mathbf{E}_1 = \mathbf{K}^\top (\mathbf{B}_I - \mathbf{A}_I) \mathbf{J}_{IF}$ and $\mathbf{E}_2 = \mathbf{K}'^\top (\mathbf{B}_I - \mathbf{A}_I) \mathbf{J}_{IF}$ such that

$$\begin{aligned} \tilde{\mu}_T^{\text{FCHT}}(t) &= \det(\mathbf{\Omega}_I) \sqrt{\frac{\det(\mathbf{A}_F)}{(2\pi i)^N}} (-i) \frac{\partial}{\partial \mathbf{E}_1} \int \int e^{\left(\frac{i}{2} \begin{bmatrix} \mathbf{Q}_F & \mathbf{Q}'_F \end{bmatrix} \mathbf{D} \begin{bmatrix} \mathbf{Q}_F \\ \mathbf{Q}'_F \end{bmatrix} + i \mathbf{E}^\top \begin{bmatrix} \mathbf{Q}_F \\ \mathbf{Q}'_F \end{bmatrix} + iF \right)} d\mathbf{Q}_F d\mathbf{Q}'_F \\ &= \det(\mathbf{\Omega}_I) \sqrt{\frac{(-2\pi i)^N \det(\mathbf{A}_F)}{\det(\mathbf{D})}} (-i) \frac{\partial}{\partial \mathbf{E}_1} e^{i \left(-\frac{\mathbf{E}^\top \mathbf{D}^{-1} \mathbf{E}}{2} + F \right)} \\ &= \det(\mathbf{\Omega}_I) \sqrt{\frac{(-2\pi i)^N \det(\mathbf{A}_F)}{\det(\mathbf{D})}} (-i) e^{i \left(-\frac{\mathbf{E}^\top \mathbf{D}^{-1} \mathbf{E}}{2} + F \right)} \left(\frac{-i}{2} \right) (\mathbf{D}^{-1} + (\mathbf{D}^{-1})^\top) \mathbf{E} \Big|_{[1:N]} \\ &= -\frac{\mu_T^{\text{FC}}(t)}{2} (\mathbf{D}^{-1} + (\mathbf{D}^{-1})^\top) \mathbf{E} \Big|_{[1:N]}, \end{aligned} \quad (51)$$

where the notation $\mathbf{u} = \mathbf{v}|_{[1:N]}$ implies that \mathbf{u} and \mathbf{v} are N and $2N$ dimensional column arrays respectively and that \mathbf{u} is the upper half of \mathbf{v} (i.e. comprised of the array elements of \mathbf{v} indexed from 1 to N).

C Derivation of the analytical expression of $\mu^{\text{HT}}(t)$

To derive $\mu_T^{\text{HT}}(t)$, we begin by plugging ρ_{if}^{HT} from Eq. (8) into $\mu_T^{\text{HT}}(t)$ from Eq. (14),

$$\mu_T^{\text{HT}}(t) = \sum_{i,f} \frac{1}{Z_I} \langle \chi_i | \left(\hat{\mathbf{R}} - \mathbf{R}_0 \right)^\top | \chi_f \rangle \nabla \vec{\gamma}^\top \nabla^\top \vec{\gamma} \langle \chi_i | \left(\hat{\mathbf{R}} - \mathbf{R}_0 \right) | \chi_f \rangle e^{-iE_i t} e^{-iE_f t}. \quad (52)$$

The previous expression may be reorganized by considering that given a vector \mathbf{v} and a matrix \mathbf{M} ,

$$\mathbf{v}^\top \mathbf{M} \mathbf{v} = \sum_{\xi\epsilon} \mathbf{v}_\xi \mathbf{M}_{\xi\epsilon} \mathbf{v}_\epsilon = \sum_{\xi\epsilon} [\mathbf{M} \circ (\mathbf{v} \mathbf{v}^\top)]_{\xi\epsilon} \quad (53)$$

where \circ denotes the Hadamard product. Consequently, we may reorganize Eq. (52) as

$$\mu_T^{\text{HT}}(t) = \sum_{\xi\epsilon} \left[[\nabla \vec{\gamma}^\top \nabla^\top \vec{\gamma}] \circ \tilde{\mu}_T^{\text{HT}}(t) \right]_{\xi\epsilon}, \quad (54)$$

where

$$\tilde{\mu}_T^{\text{HT}}(t) = \sum_{i,f} \frac{e^{-iE_i\tau} e^{-iE_f t}}{Z_I} \left[\langle \chi_f | (\hat{\mathbf{R}} - \mathbf{R}_0) | \chi_i \rangle \langle \chi_i | (\hat{\mathbf{R}} - \mathbf{R}_0)^\top | \chi_f \rangle \right] \quad (55)$$

is a square matrix whose axes have dimensions equal to the number of vibrational degrees of freedom. Eq. (55) can be rendered more compact when using

$$\sum_f e^{-i\hat{E}_f t} \langle \chi_i | (\hat{\mathbf{R}} - \mathbf{R}_0) | \chi_f \rangle \langle \chi_f | (\hat{\mathbf{R}} - \mathbf{R}_0)^\top | \chi_i \rangle = \langle \chi_i | (\hat{\mathbf{R}} - \mathbf{R}_0) e^{-i\hat{H}_F t} (\hat{\mathbf{R}} - \mathbf{R}_0)^\top | \chi_i \rangle, \quad (56)$$

so that

$$\begin{aligned} \tilde{\mu}_T^{\text{HT}}(t) &= \sum_{i,f} \frac{e^{-iE_i\tau}}{Z_I} \langle \chi_i | (\hat{\mathbf{R}} - \mathbf{R}_0) e^{-i\hat{H}_F t} (\hat{\mathbf{R}} - \mathbf{R}_0)^\top | \chi_i \rangle, \\ &= \int \int \frac{1}{Z_I} \langle \mathbf{R}' | e^{-i\hat{H}_I \tau} | \mathbf{R} \rangle \langle \mathbf{R} | (\hat{\mathbf{R}} - \mathbf{R}_0) e^{-i\hat{H}_F t} (\hat{\mathbf{R}} - \mathbf{R}_0)^\top | \mathbf{R}' \rangle d\mathbf{R} d\mathbf{R}'. \end{aligned} \quad (57)$$

Given the freedom to Taylor expand $\gamma(\mathbf{R})$ from any point, one can choose $\mathbf{R}_0 = 0$ thereby simplifying Eq. (57) into

$$\tilde{\mu}_T^{\text{HT}}(t) = \int \int \frac{1}{Z_I} \langle \mathbf{R}' | e^{-i\hat{H}_I \tau} | \mathbf{R} \rangle \langle \mathbf{R} | \hat{\mathbf{R}} e^{-i\hat{H}_F t} \hat{\mathbf{R}}^\top | \mathbf{R}' \rangle d\mathbf{R} d\mathbf{R}'. \quad (58)$$

In the coordinate representation, the term on the right-hand side in the equation above becomes

$$\begin{aligned}
\langle \mathbf{R} | \hat{\mathbf{R}} e^{-i\hat{H}t} \hat{\mathbf{R}}^\top | \mathbf{R}' \rangle &= \int \int \langle \mathbf{R} | \hat{\mathbf{R}} | \mathbf{R}'' \rangle \langle \mathbf{R}'' | e^{-i\hat{H}t} | \mathbf{R}''' \rangle \langle \mathbf{R}''' | \hat{\mathbf{R}}^\top | \mathbf{R}' \rangle d\mathbf{R}'' d\mathbf{R}''' \\
&= \int \int \delta(\mathbf{R} - \mathbf{R}'') \mathbf{R}'' \langle \mathbf{R}'' | e^{-i\hat{H}t} | \mathbf{R}''' \rangle \mathbf{R}'''^\top \delta(\mathbf{R}''' - \mathbf{R}') d\mathbf{R}'' d\mathbf{R}''' \quad (59) \\
&= \mathbf{R} \langle \mathbf{R} | e^{-i\hat{H}t} | \mathbf{R}' \rangle \mathbf{R}'^\top
\end{aligned}$$

allowing Eq. (58) to become

$$\tilde{\mu}_T^{\text{HT}}(t) = \int \int \frac{\langle \mathbf{R}' | e^{-i\hat{H}_I\tau} | \mathbf{R} \rangle}{Z_I} \mathbf{R} \langle \mathbf{R} | e^{-i\hat{H}_F t} | \mathbf{R}' \rangle \mathbf{R}'^\top d\mathbf{R} d\mathbf{R}'. \quad (60)$$

Like in Appendix B, we can replace \mathbf{R} by the normal modes \mathbf{Q} and use the result of Eq. (34) to express Eq. (60) as follows

$$\begin{aligned}
\tilde{\mu}_T^{\text{HT}}(t) &= \int \int \mathbf{Q}_F \mathbf{Q}_F'^\top |\Omega_I| \sqrt{\frac{\det(\mathbf{A}_F)}{(2\pi i)^N}} e^{\left(-\frac{i}{2} \begin{bmatrix} \mathbf{Q}_F & \mathbf{Q}_F' \end{bmatrix} \mathbf{D} \begin{bmatrix} \mathbf{Q}_F \\ \mathbf{Q}_F' \end{bmatrix} + i\mathbf{E}^\top \begin{bmatrix} \mathbf{Q}_F \\ \mathbf{Q}_F' \end{bmatrix} + iF \right)} d\mathbf{Q}_F d\mathbf{Q}_F' \\
&= -\frac{\partial}{\partial \mathbf{E}_1} \left(\frac{\partial}{\partial \mathbf{E}_2} \right)^\top \tilde{\mu}_T^{\text{FC}}(t) \\
&= -\tilde{\mu}_T^{\text{FC}}(t) \left[\left[(\mathbf{d}_{11} + \mathbf{d}_{11}^\top) \mathbf{E}_1 + (\mathbf{d}_{12} + \mathbf{d}_{12}^\top) \mathbf{E}_2 \right] \left[\mathbf{E}_2^\top (\mathbf{d}_{22} + \mathbf{d}_{22}^\top) + \mathbf{E}_1^\top (\mathbf{d}_{21} + \mathbf{d}_{12}) \right] + i(\mathbf{d}_{12}^\top + \mathbf{d}_{12}) \right], \quad (61)
\end{aligned}$$

where we have defined

$$\begin{bmatrix} \mathbf{d}_{11} & \mathbf{d}_{12} \\ \mathbf{d}_{21} & \mathbf{d}_{22} \end{bmatrix} = \frac{\mathbf{D}^{-1}}{2}. \quad (62)$$

D The time-discontinuity of propagators from the path integral (PI) formalism

The origin of the discontinuity in propagators is well documented and can be found in many textbooks.^{28–30} Within the PI formulation, the propagator of one-dimension system is given

as $\langle q|e^{-i\hat{H}t'}|q'\rangle = \int_0^{t'} e^{iS[\mathbf{q}]} \mathcal{D}\mathbf{q}$ where $S[\mathbf{q}]$ denotes the action of a trajectory $\mathbf{q} = \mathbf{q}(t)$, $\int_0^{t'} \mathcal{D}\mathbf{q}$ denotes integration over all trajectories with $\mathbf{q}(0) = q$ and $\mathbf{q}(t') = q'$.

By applying the semiclassical approximation, which consists in Taylor expanding $S[\mathbf{q}]$ around the classical trajectory \mathbf{q}_c , the propagator can be approximated by the following factorized form

$$\langle q|e^{-i\hat{H}t'}|q'\rangle \approx e^{iS[\mathbf{q}_c]} \int_0^{t'} e^{\frac{i}{2}\delta^2 S[\delta\mathbf{q}]} \mathcal{D}\delta\mathbf{q}, \quad (63)$$

where $\int \mathcal{D}\delta\mathbf{q}$ denotes integration over variations $\delta\mathbf{q} = \delta\mathbf{q}(t)$, which are subject to boundary conditions $\delta\mathbf{q}(0) = 0$ and $\delta\mathbf{q}(t') = 0$. The integral term in Eq. (63) is often referred to as the *fluctuation factor*²⁹ and in the case of the harmonic oscillator it coincides with the pre-exponential factor in Eq. (18), the root of the time-discontinuity. The second functional derivative of the action

$$\Lambda = \frac{\delta^2 S[\mathbf{q}_c]}{\delta\mathbf{q}\delta\mathbf{q}'} = -m \frac{d^2}{dt^2} - \frac{\partial^2 V[\mathbf{q}_c]}{\partial\mathbf{q}^2}, \quad (64)$$

is needed to evaluate the second variation $\delta^2 S[\delta\mathbf{x}]$.

To do so, a common approach⁵⁰ consists in expanding $\delta\mathbf{q}$ in the basis of the eigenfunctions of Λ , $\Lambda u_n(t) = \lambda_n u_n(t)$ subject to boundary conditions $u_n(0) = u_n(t') = 0$. In the case of the harmonic oscillator, this amounts to a Fourier expansion

$$\delta\mathbf{q}(t) = \sum_{n=1}^{\infty} a_n u_n(t) = \sum_{n=1}^{\infty} a_n \sqrt{\frac{2}{t'}} \sin\left(\frac{n\pi t}{t'}\right), \quad (65)$$

which results in the fluctuation factor being proportional to $\prod_{n=1}^{\infty} \lambda_n^{-1/2}$ where $\lambda_n = m \left[\left(\frac{n\pi}{t'}\right)^2 - w^2 \right]$. The term λ_n can be interpreted to be the curvature of $S[\mathbf{q}]$ near \mathbf{q}_c along the direction $u_n(t)$. All λ_n starts off by being positive before becoming negative after their half-periods. The classical harmonic trajectory minimizes the action when $t' < \frac{\pi}{w}$ and becomes a saddle point when $t' > \frac{\pi}{w}$. Ultimately, this switch is the reason behind the discontinuity of $\bar{\mu}_T^{\text{FC}}(t)$.

References

- (1) Ruhoff, P. T. Recursion relations for multi-dimensional Franck-Condon overlap integrals. *Chem. Phys.* **1994**, *186*, 355–374.
- (2) Dierksen, M.; Grimme, S. An efficient approach for the calculation of Franck-Condon integrals of large molecules. *J. Chem. Phys.* **2005**, *122*, 244101.
- (3) Santoro, F.; Improta, R.; Lami, A.; Bloino, J.; Barone, V. Effective method to compute Franck-Condon integrals for optical spectra of large molecules in solution. *J. Chem. Phys.* **2007**, *126*, 084509.
- (4) Chang, J.-L. A new method to calculate Franck-Condon factors of multidimensional harmonic oscillators including the Duschinsky effect. *J. Chem. Phys.* **2008**, *128*, 174111.
- (5) Heller, E. J. The semiclassical way to molecular spectroscopy. *Acc. Chem. Res.* **1981**, *14*, 368–375.
- (6) Niu, Y.; Peng, Q.; Deng, C.; Gao, X.; Shuai, Z. Theory of excited state decays and optical spectra: application to polyatomic molecules. *J. Phys. Chem. A* **2010**, *114*, 7817–7831.
- (7) Peng, Q.; Niu, Y.; Deng, C.; Shuai, Z. Vibration correlation function formalism of radiative and non-radiative rates for complex molecules. *Chem. Phys.* **2010**, *370*, 215–222.
- (8) Baiardi, A.; Bloino, J.; Barone, V. General time dependent approach to vibronic spectroscopy including Franck-Condon, Herzberg-Teller, and Duschinsky effects. *J. Chem. Theory Comput.* **2013**, *9*, 4097–4115.
- (9) de Souza, B.; Neese, F.; Izsák, R. On the theoretical prediction of fluorescence rates from first principles using the path integral approach. *J. Chem. Phys.* **2018**, *148*, 034104.

- (10) Begušić, T.; Van íček, J. On-the-fly ab initio semiclassical evaluation of vibronic spectra at finite temperature. *J. Chem. Phys.* **2020**, *153*, 024105.
- (11) Jacquemin, D.; Brémond, E.; Planchat, A.; Ciofini, I.; Adamo, C. TD-DFT vibronic couplings in anthraquinones: from basis set and functional benchmarks to applications for industrial dyes. *J. Chem. Theory Comput.* **2011**, *7*, 1882–1892.
- (12) Huh, J.; Guerreschi, G. G.; Peropadre, B.; McClean, J. R.; Aspuru-Guzik, A. Boson sampling for molecular vibronic spectra. *Nature Photonics* **2015**, *9*, 615–620.
- (13) Ryabinkin, I. G.; Yen, T.-C.; Genin, S. N.; Izmaylov, A. F. Qubit coupled cluster method: a systematic approach to quantum chemistry on a quantum computer. *J. Chem. Theory Comput.* **2018**, *14*, 6317–6326.
- (14) Duschinsky, F. The importance of the electron spectrum in multi atomic molecules. Concerning the Franck-Condon principle. *Acta Physicochim. URSS* **1937**, *7*, 551–566.
- (15) Domcke, W.; Cederbaum, L.; Köppel, H.; Von Niessen, W. A comparison of different approaches to the calculation of franck-condon factors for polyatomic molecules. *Mol. Phys.* **1977**, *34*, 1759–1770.
- (16) Hazra, A.; Chang, H. H.; Nooijen, M. First principles simulation of the UV absorption spectrum of ethylene using the vertical Franck-Condon approach. *J. Chem. Phys.* **2004**, *121*, 2125–2136.
- (17) Ferrer, F. J. A.; Santoro, F. Comparison of vertical and adiabatic harmonic approaches for the calculation of the vibrational structure of electronic spectra. *Phys. Chem. Chem. Phys.* **2012**, *14*, 13549–13563.
- (18) Cerezo, J.; Zuniga, J.; Requena, A. Harmonic models in cartesian and internal coordinates to simulate the absorption spectra of carotenoids at finite temperatures. *J. Chem. Theory Comput.* **2013**, *9*, 4947–4958.

- (19) Petrenko, T.; Neese, F. Efficient and automatic calculation of optical band shapes and resonance Raman spectra for larger molecules within the independent mode displaced harmonic oscillator model. *J. Chem. Phys.* **2012**, *137*, 234107.
- (20) Ianconescu, R.; Pollak, E. Photoinduced cooling of polyatomic molecules in an electronically excited state in the presence of Dushinskii rotations. *J. Phys. Chem. A* **2004**, *108*, 7778–7784.
- (21) Baiardi, A.; Bloino, J.; Barone, V. General formulation of vibronic spectroscopy in internal coordinates. *J. Chem. Phys.* **2016**, *144*, 084114.
- (22) Benkyi, I.; Tapavicza, E.; Fliegl, H.; Sundholm, D. Calculation of vibrationally resolved absorption spectra of acenes and pyrene. *Phys. Chem. Chem. Phys.* **2019**, *21*, 21094–21103.
- (23) Begušić, T.; Tapavicza, E.; Van’iček, J. Applicability of the Thawed Gaussian Wavepacket Dynamics to the Calculation of Vibronic Spectra of Molecules with Double-Well Potential Energy Surfaces. *J. Chem. Theory Comput.* **2022**, *18*, 3065.
- (24) Tapavicza, E.; Furche, F.; Sundholm, D. Importance of vibronic effects in the UV–Vis spectrum of the 7, 7, 8, 8-tetracyanoquinodimethane anion. *J. Chem. Theory Comput.* **2016**, *12*, 5058–5066.
- (25) Horváthy, P. A. The Maslov correction in the semiclassical Feynman integral. *Cent. Eur. J. Phys.* **2011**, *9*, 1–12.
- (26) Thornber, N. S.; Taylor, E. F. Propagator for the simple harmonic oscillator. *Am. J. Phys.* **1998**, *66*, 1022–1024.
- (27) Rosenfelder, R. On the numerical evaluation of real-time path integrals: Double exponential integration and the Maslov correction. e-print *arXiv:2105.02880* [physics] **2021**, <https://doi.org/10.48550/arXiv.2105.02880> (accessed 2022-05-12).

- (28) Tannor, D. J. *Introduction to Quantum Mechanics: a Time-Dependent Perspective*; University Science Books: Sausalito, CA, USA, 2007; p 437.
- (29) Kleinert, H. *Path Integrals in Quantum Mechanics, Statistics, Polymer Physics, and Financial Markets*; World scientific: Singapore, 2009; p 104.
- (30) Schulman, L. S. *Techniques and Applications of Path Integration*; Courier Corporation: Mineola, NY, USA, 2012; p 143.
- (31) Schatz, G. C.; Ratner, M. A. *Quantum Mechanics in Chemistry*; Courier Corporation: Mineola, NY, USA, 2002; pp 73, 201.
- (32) Domcke, W.; Yarkony, D.; Köppel, H. *Conical Intersections: Electronic Structure, Dynamics & Spectroscopy*; World Scientific: Singapore, 2004; Vol. 15; p 704.
- (33) Powell, P. D. Calculating determinants of block matrices. e-print *arXiv:1112.4379* [math] **2011**, <https://doi.org/10.48550/arXiv.1112.4379> (accessed 2022-03-15).
- (34) Granovsky, A. A. Firefly version 8. <http://classic.chem.msu.su//gran/firefly/index.html>, Accessed: 2022-01-03.
- (35) Becke, A. D. A new mixing of Hartree–Fock and local density-functional theories. *J. Chem. Phys.* **1993**, *98*, 1372–1377.
- (36) Lee, C.; Yang, W.; Parr, R. G. Development of the Colle-Salvetti correlation-energy formula into a functional of the electron density. *Phys. Rev. B* **1988**, *37*, 785.
- (37) Ditchfield, R.; Hehre, W. J.; Pople, J. A. Self-consistent molecular-orbital methods. IX. An extended Gaussian-type basis for molecular-orbital studies of organic molecules. *J. Chem. Phys.* **1971**, *54*, 724–728.
- (38) Cerezo, J.; Santoro, F. Revisiting vertical models to simulate the line shape of electronic spectra adopting Cartesian and internal coordinates. *J. Chem. Theory Comput.* **2016**, *12*, 4970–4985.

- (39) Harris, C. R.; Millman, K. J.; van der Walt, S. J.; Gommers, R.; Virtanen, P.; Cournapeau, D.; Wieser, E.; Taylor, J.; Berg, S.; Smith, N. J. et al. Array programming with NumPy. *Nature* **2020**, *585*, 357–362.
- (40) Halasinski, T. M.; Hudgins, D. M.; Salama, F.; Allamandola, L. J.; Bally, T. Electronic absorption spectra of neutral pentacene (C₂₂H₁₄) and its positive and negative ions in Ne, Ar, and Kr matrices. *J. Phys. Chem. A* **2000**, *104*, 7484–7491.
- (41) Thusek, J.; Hoffmann, M.; Hübner, O.; Germer, S.; Hoffmann, H.; Freudenberg, J.; Bunz, U. H.; Dreuw, A.; Himmel, H.-J. High-Resolution Electronic Excitation and Emission Spectra of Pentacene and 6, 13-Diazapentacene Monomers and Weakly Bound Dimers by Matrix-Isolation Spectroscopy. *Chemistry* **2021**, *27*, 2072.
- (42) Adamo, C.; Scuseria, G. E.; Barone, V. Accurate excitation energies from time-dependent density functional theory: Assessing the PBE0 model. *J. Chem. Phys.* **1999**, *111*, 2889–2899.
- (43) Berger, R.; Fischer, C.; Klessinger, M. Calculation of the vibronic fine structure in electronic spectra at higher temperatures. 1. benzene and pyrazine. *J. Phys. Chem. A* **1998**, *102*, 7157–7167.
- (44) Bernhardsson, A.; Forsberg, N.; Malmqvist, P.-Å.; Roos, B. O.; Serrano-Andrés, L. A theoretical study of the 1 B 2u and 1 B 1u vibronic bands in benzene. *J. Chem. Phys.* **2000**, *112*, 2798–2809.
- (45) Schumm, S.; Gerhards, M.; Kleinerhanns, K. Franck-Condon simulation of the S₁→S₀ spectrum of Phenol. *J. Phys. Chem. A* **2000**, *104*, 10648–10655.
- (46) Li, J.; Lin, C.-K.; Li, X. Y.; Zhu, C. Y.; Lin, S. H. Symmetry forbidden vibronic spectra and internal conversion in benzene. *Phys. Chem. Chem. Phys.* **2010**, *12*, 14967–14976.

- (47) He, R.; Yang, L.; Zhu, C.; Yamaki, M.; Lee, Y.-P.; Lin, S. H. Franck–Condon simulation of the $A\ 1\ B\ 2 \rightarrow X\ 1\ A\ 1$ dispersed fluorescence spectrum of fluorobenzene and its rate of the internal conversion. *J. Chem. Phys.* **2011**, *134*, 094313.
- (48) Taniguchi, M.; Du, H.; Lindsey, J. S. PhotochemCAD 3: diverse modules for photo-physical calculations with multiple spectral databases. *Photochem. Photobiol.* **2018**, *94*, 277–289.
- (49) Huh, J.; Berger, R. Cumulant expansion for fast estimate of non-Condon effects in vibronic transition profiles. *Sci. Rep.* **2017**, *7*, 1–8.
- (50) Feynman, R. P.; Hibbs, A. R.; Styer, D. F. *Quantum Mechanics and Path Integrals*; Courier Corporation: Mineola, NY, USA, 2010.

TOC Graphic

